Electromagnetic Wave Scattering From Sea and Bare Soil Surfaces Based On An Improved Two-Scale Model

Naheed SAJJAD, Ali KHENCHAF, Arnaud COATANHAY
ENSIETA/E3I2-Laboratory
2 rue Francois Verny, 29806, Brest Cedex 09,France
{naheed.sajjad, ali.khenchaf, arnaud.coatanhay}@ensieta.fr

Abstract— **Remote sensing applications require developing accurate models to predict radar backscattering from rough surfaces. An improved two-scale model to calculate the electromagnetic backscattering coefficients from sea and bare soil surface is investigated. The sea surface calculations are made by assuming the surface height spectrum of Elfouhaily et al. whereas the roughness of soil surface is approximated by Gaussian spectrum. The simulation results are compared with the published experimental data from ocean surface at Ku-band and for soil surface at L-band. Fairly good agreements are found for the fixed physical surface roughness parameters on these frequency bands specially, for cross polarizations. It is observed that as the roughness of the surface increases the intensity of σ_{HH} increases at low grazing angles.**

Keywordst; two scale model, rough sea surface, soil rough surface, low grazing angles

I. INTRODUCTION

Radar backscattering response of ocean and soil surfaces can be used to retrieve the surface parameters like the wind speed and wind direction, root mean square (rms) surface height, correlation length, AutoCorrelation Function (ACF) and soil moisture. To analyze the wave scattering from these surfaces with random roughness analytically, the approximate solutions of Kirchhoff Approximation (KA) [1], Small Perturbation Method (SPM) [2, 3], the Phase Perturbation Technique (PPT) [4], the Two Scale Model (TSM) [5, 6, 7] and the Small Slope Approximation (SSA) [8, 9] were usually used. However, these methods have restricted domain of validity.

For electromagnetic scattering from sea and soil surface, TSM can be used by splitting the surface into two scales [2, 10]: a large and small one related to the incident wave. The classical TSM use the KA for the large scale and a first order SPM (SPM1) for the small scale [5]. Historically normalized radar cross section of vertical polarization σ_{VV} has been known to be rather well explained by Bragg scattering augmented by a composite, or two-scale, rough surface over the range of incidence angles from approximately 20° to 60° and probably at even higher incidence angles, into the so called LGA regime [11, 12]. On the other hand, there is a need to study σ_{HH} in more detail. It is appeared to be fairly well predicted by Bragg/TSM surface scattering from 20° to 45° incidence but at larger incident angles this intensity is considerably stronger than that expected from theoretical computation. Moreover, the predictions for cross-polarization by TSM in backscattering are not exact which in essence is the factual problem, as for soil surface applications the intensity of σ_{HV} is used to better estimate the soil parameters [13].

To get improved intensity of σ_{HH} at larger incident angles and better predictions of σ_{HV}, an improved TSM have been proposed [14] by taking into account the contribution of second order scattering effects into the first order at small scale. To capture the features exhibited by sea scattering Cox & Munk slope distribution [15] and a roughness spectrum obtained from the Elfouhaily et al. for fully developed seas [16] is used. For sea surface, we investigate the improved TSM at L-, C- and Ku-band with wind speeds of 7m/s and 15m/s. The performance of this model has been assessed by comparing the numerical results with experimental data [17, 21] at Ku-band. The application of this model is then extended for soil surface by using Gaussian spectrum. The simulations for soil surface have been performed for L-band and compared with measured data [18] at two roughness levels. For both surfaces, good predictions are found for σ_{HV} and we observe that as the roughness of surfaces increases the intensity of σ_{HH} improves up to 5dB from moderate to larger incident angles.

The rest of the paper is organized as follows: in section II we introduce the theoretical development of improved TSM, in section III, the sea and soil surface description based on slope distribution and spectrum models are cited shortly, section IV include the simulation results and comparisons for both surfaces. Finally, the conclusions and prospectives of this work are reported.

II. DIFFUSION MODEL

This section contains a small review of KA and SPM up to second order and then an improved two scale model is presented. Geometrical configuration adapted to resolve the wave-scattering problem given in Fig. 1.

KA approach [1] assumes that the rough surface can be approximated by a tangent plane at each point of the surface. It is only valid for a surface with an important horizontal roughness scale and average radius of curvature compared to the electromagnetic wavelength. This approach is well adapted

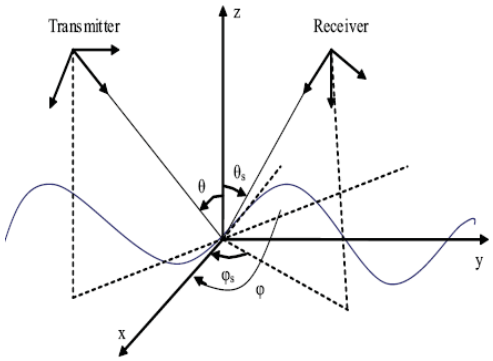

Figure 1. Geometrical representation of bistatic configuration

to the computation of the specular component.

For SPM we use the formulation given by Tsang [19]. The extended boundary condition method, which relates the surface tangential fields to the incident fields, is used to solve the surface field parameters to second order for small rms height. Here we summarize the results and refer readers to [19] for the detailed SPM formulation and derivation. For an electromagnetic wave scattered by a dielectric rough surface, the first order bistatic scattering coefficient and the correlation product can be written as

$$\sigma_{mn}^{(1)} = 4\pi k^2 \cos\theta_s W\left(\bar{k}_{s\perp} - \bar{k}_{i\perp}\right) f_{mn}^{(1)}\left(\bar{k}_{s\perp}, \bar{k}_{i\perp}\right) \quad (1)$$

$$\sigma_{pqmn}^{(1)} = 8\pi k^2 \cos^2\theta_s W\left(\bar{k}_{s\perp} - \bar{k}_{i\perp}\right) \mathrm{Re}\left(f_{pq}^{(1)}\left(\bar{k}_{s\perp}, \bar{k}_{i\perp}\right) . f_{mn}^{(1)*}\left(\bar{k}_{s\perp}, \bar{k}_{i\perp}\right)\right) \quad (2)$$

where $\bar{k}_\perp$ denotes vector $k_x\hat{x} + k_y\hat{y}$ in (x,y)-plane, $W\left(\bar{k}_{s\perp} - \bar{k}_{i\perp}\right)$ is the spectrum and $f_{mn}^{(1)}$ are the first order polarization dependent coefficients. The second order bistatic scattering coefficient and the correlation product is given by

$$\sigma_{mn}^{(2)} = 4\pi k^2 \cos^2\theta_s \left(\int_{-\infty}^{\infty} d\bar{k}_\perp^{\cdot} W\left(\bar{K}_{s\perp} - \bar{K}_\perp^{\cdot}\right) W\left(\bar{K}_\perp^{\cdot} - \bar{K}_{i\perp}\right) f_{mn}^{(2)}\left(\bar{k}_{s\perp}, \bar{k}_\perp^{\cdot}, \bar{k}_{i\perp}\right)\left[f_{mn}^{(2)*}\left(\bar{k}_{s\perp}, \bar{k}_\perp^{\cdot}, \bar{k}_{i\perp}\right) + f_{mn}^{(2)*}\left(\bar{k}_{s\perp}, \bar{k}_{s\perp} - \bar{k}_\perp^{\cdot} + \bar{k}_{i\perp}, \bar{k}_{i\perp}\right)\right]\right) \quad (3)$$

$$\sigma_{pqmn}^{(2)} = 4\pi k^2 \cos^2\theta_s \left(\int_{-\infty}^{\infty} d\bar{k}_\perp^{\cdot} W\left(\bar{k}_{s\perp} - \bar{k}_\perp^{\cdot}\right) W\left(\bar{k}_\perp^{\cdot} - \bar{k}_{i\perp}\right) . f_{pq}^{(2)}\left(\bar{k}_{s\perp}, \bar{k}_\perp^{\cdot}, \bar{k}_{i\perp}\right)\left[f_{mn}^{(2)*}\left(\bar{k}_{s\perp}, \bar{k}_\perp^{\cdot}, \bar{k}_{i\perp}\right) + f_{mn}^{(2)*}\left(\bar{k}_{s\perp}, \bar{k}_{s\perp} - \bar{k}_\perp^{\cdot} + \bar{k}_{i\perp}, \bar{k}_{i\perp}\right)\right]\right) \quad (4)$$

SPM is used to obtain the scattering coefficients of a slightly rough surface. The first order SPM approach provides an estimation of the diffuse component of the electromagnetic scattered wave. For monostatic case it does not predict the cross-polarized components. Its development to the second order gives estimation of co- and cross-polarized components in all directions.

The key idea of TSM is to take advantages of the classic approaches (SPM1 and KA) to enlarge the application domain [6]. In a reasonable way, sea and soil roughness can be split in to two scales: large and a small with the incident electromagnetic wavelength (Fig.2). Then scattering coefficients are estimated in two steps: firstly, the classical TSM uses SPM1 on small scale waves and then determine the diffuse component in the global reference by a tilting process.

The bistatic scattering coefficient σ_{pq} as a function of the transmitter polarization q and receiver polarization p is given by [5, 6]

$$\begin{aligned}\sigma^s_{pq} = \Big\langle &\left(p.v_s'\right)^2\left(q.v'\right)^2\sigma_{v_s'v'} + \left(p.v_s'\right)^2\left(q.h'\right)^2\sigma_{v_s'h'} \\ &+\left(p.h_s'\right)^2\left(q.v'\right)^2\sigma_{h_s'v'} + \left(p.h_s'\right)^2\left(q.h'\right)^2\sigma_{h_s'h'} \\ &+\left(p.h_s'\right)^2\left(q.v'\right)\left(q.h'\right)\sigma_{h_s'h'h_s'v'} + \left(p.v_s'\right)\left(p.h_s'\right) \\ &\left(q.h'\right)^2\sigma_{h_s'h'v_s'h'} + \left(p.v_s'\right)\left(p.h_s'\right)\left(q.h'\right)\left(q.v'\right)\sigma_{h_s'v'v_s'h'} \\ &+\left(p.v_s'\right)\left(p.h_s'\right)\left(q.h'\right)\left(q.v'\right)\sigma_{v_s'v'h_s'h'} + \left(p.v_s'\right)^2\left(p.h_s'\right) \\ &\left(q.v'\right)^2\sigma_{h_s'v'v_s'v'} + \left(p.h_s'\right)^2\left(q.v'\right)\left(q.h'\right)\sigma_{v_s'v'v_s'h'}\Big\rangle \end{aligned} \quad (5)$$

where h', v', h_s' and v_s' are the local, incident and scattered polarizations. $\sigma_{p'q'}$ and $\sigma_{p'q'm'n'}$ are obtained from (1) & (2) by using SPM1and calculated at local angles. The average $\langle . \rangle$ with respect to large-scale roughness can be weighted by using surface slope model.

We have proposed an improved TSM by adding the SPM2 correction to SPM1 i.e.,

$$\begin{cases} \sigma_{p'q'} = \sigma_{p'q'}^{(1)} + \sigma_{p'q'}^{(2)} \\ \sigma_{p'q'm'n'} = \sigma_{p'q'm'n'}^{(1)} + \sigma_{p'q'm'n'}^{(2)} \end{cases} \quad (6)$$

For complete second order scattering contribution one must calculate third order field $E_s^{(3)}$., but it involves complication for three dimensional problems. The simulation results based on this model are given in section IV along with comparisons with experimental data and other diffusion models (Classic TSM, SPM1 and SPM1+SPM2).

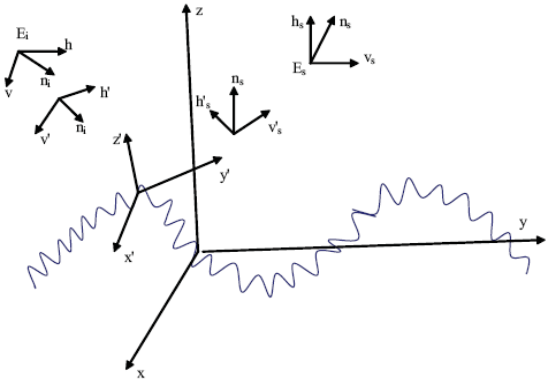

Figure 2. Geometry of a surface bistatic scattering in the two-scale model

III. ROUGH SURFACE DESCRIPTION

The scattering properties of the rough surface depend both on its electromagnetic characteristics and its shape. To capture these properties, the models used for sea and soil surface are briefly described as follows.

A. Sea Surface

The sea surface is assumed to be non magnetic and the dielectric constant is calculated by using Debye's model [20].

As for the geometric properties we use the semi empirical slope distribution law given by Cox and Munk [15]. This probability density function is given as a function of wind speed and direction and illustrates the skewness phenomenon so it stands out as the only realistic sea slope distribution.

Among the several sea spectrum models published in the literature, we use the spectrum proposed by Elfouhaily et al [6]. This model was developed solely from in situ or tank measurements, along with physical arguments but it also agree with the slope model proposed by Cox and Munk and with actual remote sensing data. Elfouhaily et al assume a directional spectrum $W(K,\phi)$ defined in polar coordinates as

$$W(K,\phi) = W(K)\, f(K,\phi) \qquad (7)$$

where

$$W(K) = (B_L + B_H)/K^3 \qquad (8)$$

$$f(K,\phi) = [1+\Delta(K)\cos(2\phi)]/2\pi \qquad (9)$$

In (3), $W(K)$ denotes the non-directional spectrum (isotropic part) modulated by the $f(K,\phi)$ spreading function. In (4), B_L and B_H are the respective contributions from low (gravity waves) and high (capillary waves) wave numbers. ϕ is the azimuthal angle measured with respect to the mean wind direction. $\Delta(K)$ is recognized as the coefficient of the second harmonic when truncating the Fourier series expansion of $f(K,\phi)$. We have used this spectrum in sea surface simulations. Figs. 3 and 4 respectively show the fully developed isotropic unified spectrum and the unified spreading function behaviour for different wind velocities.

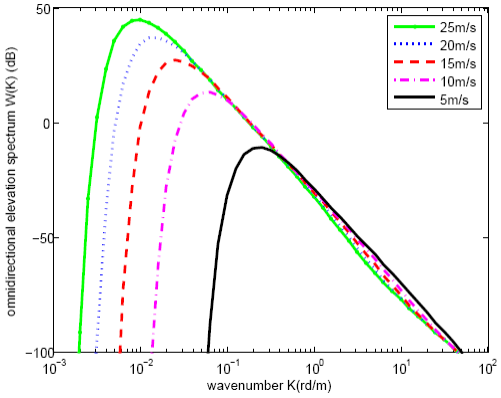

Figure 3. Elfouhaily omni directional spectra for different wind speeds

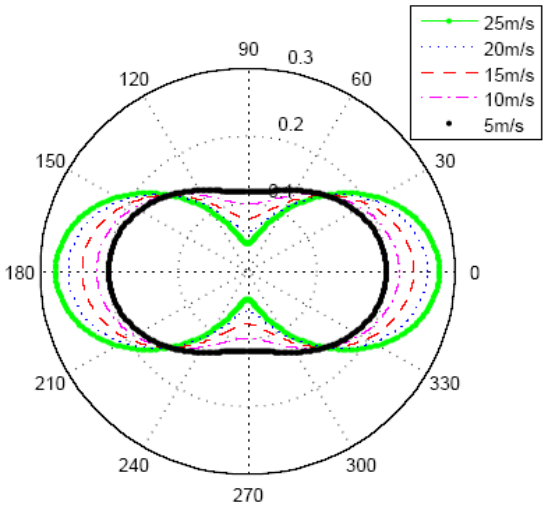

Figure 4. Elfouhaily sea surface angular function with different windspeeds

B. Bare soil surface

Again we assume that the bare soil surface is non magnetic and the value of relative permittivity is taken as and for wet soil surface [18].

Both the slope probability density function and soil spectrum is taken as Gaussian. The expression for slope pdf is given by

$$P(Z_x, Z_y) = \frac{1}{2\pi m^2}\exp\left(-\frac{Z_x^2 + Z_y^2}{2m^2}\right) \qquad (10)$$

where Z_x and Z_y are slopes in x and y direction and $m = \sqrt{2}s/l$ .The expression for Gaussian spectrum is given as

$$W(\bar{k}_\perp) = \frac{s^2 l^2}{4\pi}\exp\left(-\frac{(k_x^2 + k_y^2)l^2}{4}\right) \qquad (11)$$

where k_x and k_y are components of wave vector and l is the correlation length.

IV. NUMERICALS RESULTS

A. Sea Surface

Before simulating scattering coefficients on different frequency bands a comparison with literature is shown to validate our model [14].

The Fig. 5 (Left) deals with the effect of incidence angle on the scattering coefficients. The incident angle is equal to reception angle and the corresponding azimuth difference equals to π. The electromagnetic frequency is fixed to 13.9 GHz (Ku-band), with the wind speed set to 15 m/s and then putting it to 7 m/s (Fig. 6) at 10 meters altitude above the sea surface. The emitter is supposed to be in the downwind direction. The results by improved TSM are compared with experimental data (Right) [21], SSA (for horizontal and vertical polarization) and classic TSM (for cross polarization).

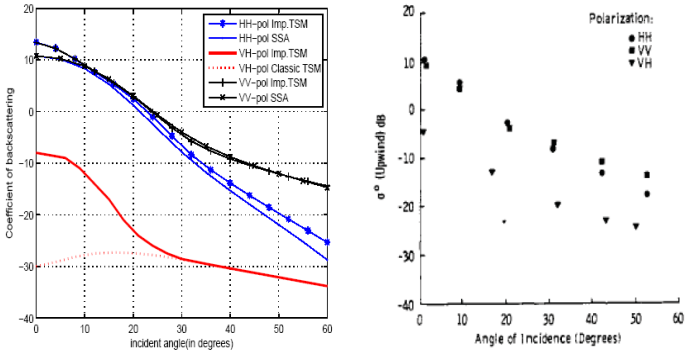

Figure 5. Comparison of Improved TSM with experimental data [21], SSA and classic TSM for cross polarization. F=13.9, wind speed=15m/s (at 10m).

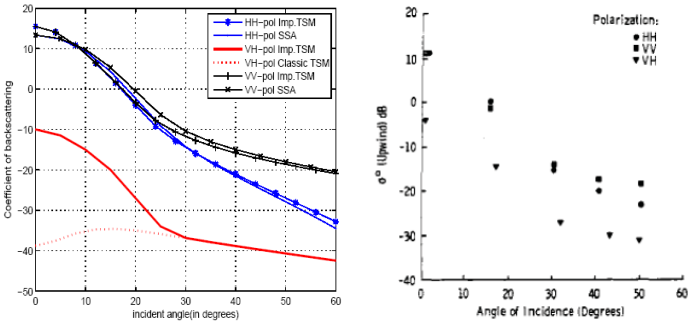

Figure 6. Comparison of Improved TSM with experimental data [21], SSA and classic TSM for cross polarization. F=13.9, wind speed=7m/s (at 10m).

Numerical simulations of scattering coefficients underline the improved TSM validity in specular and diffuse domain especially for cross polarizations. Note that the above simulation results are obtained by using composite improved TSM i. e., the specular component is calculated by KA whereas in the following simulations we used the simple improved TSM described in this paper.

Next, backscattering coefficients σ_{HH} and σ_{HV} are plotted in figures 7, 8, 9 and 10 respectively as a function of incident angle from 55° to 88°. The frequency is again fixed to 13.9 GHz and the wind speed is setup to 15 m/s and then to 7 m/s. The results are compared with the experimental data [17], sum of SPM1 and SPM1 and with classic TSM [6].

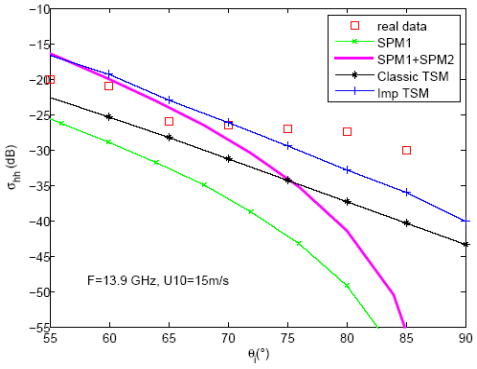

Figure 7. Comparison of Improved TSM with experimental data [17], SPM1+SPM2 and classic TSM for horizontal polarization.

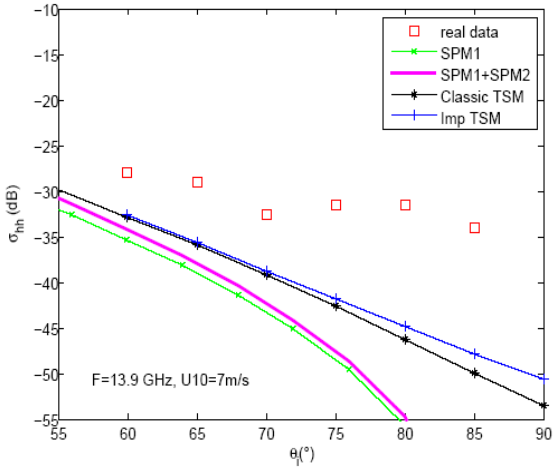

Figure 8. Comparison of Improved TSM with experimental data [17], SPM1+SPM2 and classic TSM for horizontal polarization.

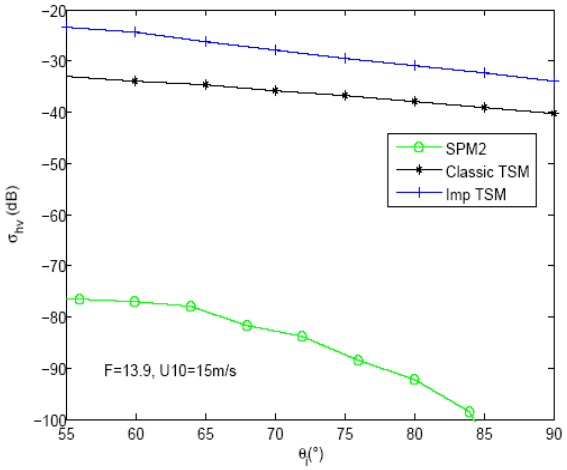

Figure 9. Comparison of Improved TSM with SPM2 and classic TSM for cross polarization. F=13.9, wind speed=15m/s (at 10m).

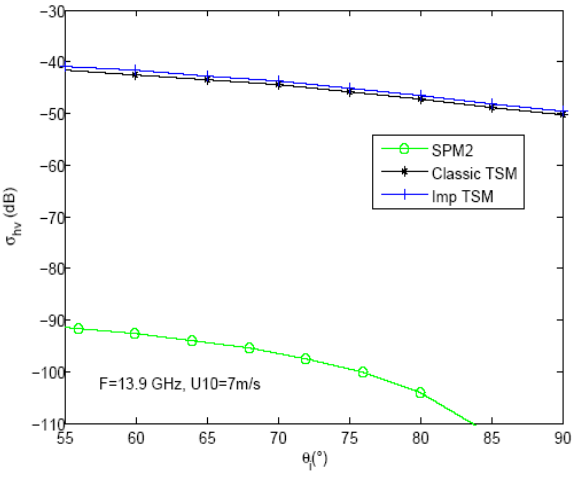

Figure 10. Comparison of Improved TSM with SPM2 and classic TSM for cross polarization. F=13.9, wind speed=7m/s (at 10m).

We observe that an improvement up to 5dB is achieved at very low grazing angles for higher wind speed (i.e., when U10=15 m/s) and the results are in good agreement with measurements for σ_{HH}. For lower wind speed (U10=7 m/s) there is no significant difference between the results of classical TSM and improved TSM and both models underestimate σ_{HH}on the LGA domain. Fig. 11 shows that for σ_{HH} behaves in a same manner on C-band (f= 4.45GHz) and L-band (f=1.5 GHz).

B. Bare Soil Surface

In this part, we extend the application of improved TSM in case of bare soil surface. We compare the backscattering coefficients of natural soil surfaces calculated from the improved TSM model by using Gaussian spectrum with the experimental data [9].

The backscattering coefficients σ_{HH} and σ_{HV} are plotted for soil surface in figures 12 and 13 respectively. The electromagnetic frequency is fixed to 1.5 GHz (L- band), the rms height is 0.4 cm and correlation length of the surface is 8.4 cm. The value of dielectric constant is taken as 15.57 [18].

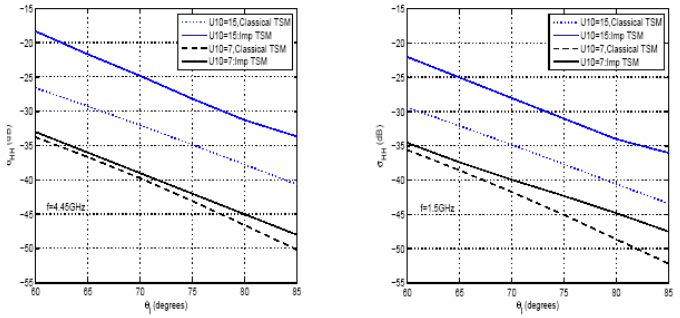

(a)F=5.3 Ghz(C-band) (b)F=1.5 GHz (L-band)

Figure 11. Comparison of Improved TSM with classic TSM for horizontal polarization at L-band (f=1.5 GHz) and C-band (f=4.45 GHz) with wind speed of 15 m/s & 7 m/s (at 10m).

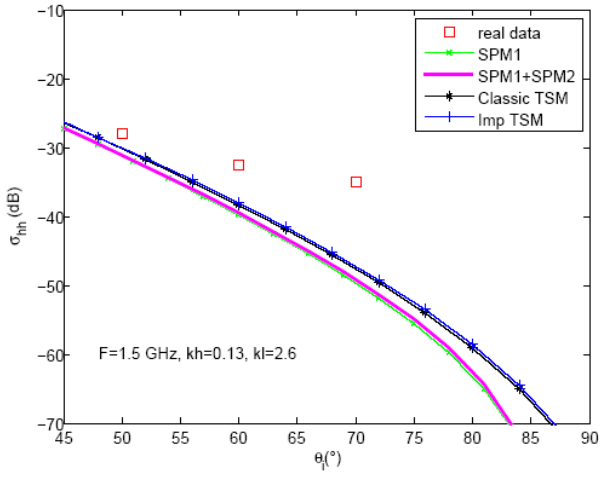

Figure 12. Comparison of Improved TSM with experimental data [18], SPM1+SPM2 and classic TSM for horizontal polarization.

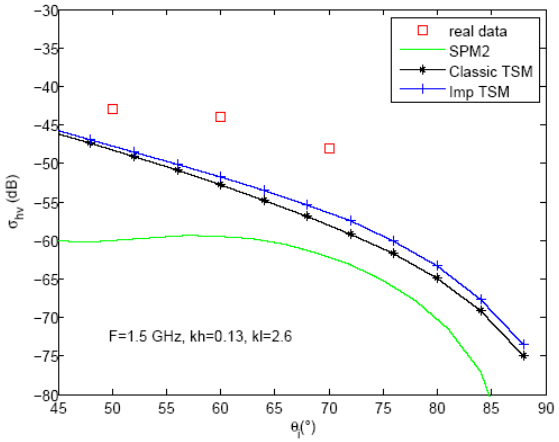

Figure 13. Comparison of Improved TSM with experimental data [18], SPM2 and classic TSM for cross polarization.

Figures 14 and 15 are plotted for σ_{HH} and σ_{HV} respectively, for relatively more rough surface on L-band with rms height set to 3.02 cm, correlation length to 8.8 and dielectric constant to 8.92.

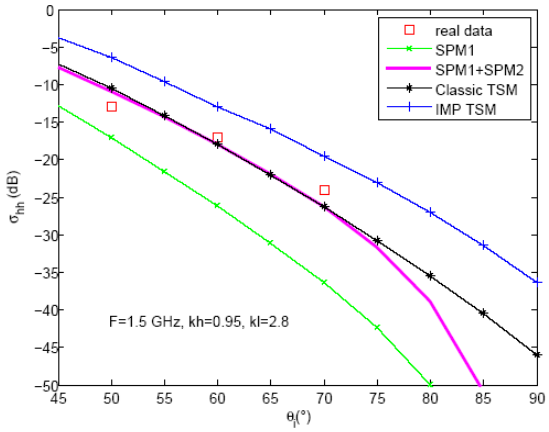

Figure 14. Comparison of Improved TSM with experimental data [18], SPM1+SPM2 and classic TSM for horizontal polarization.

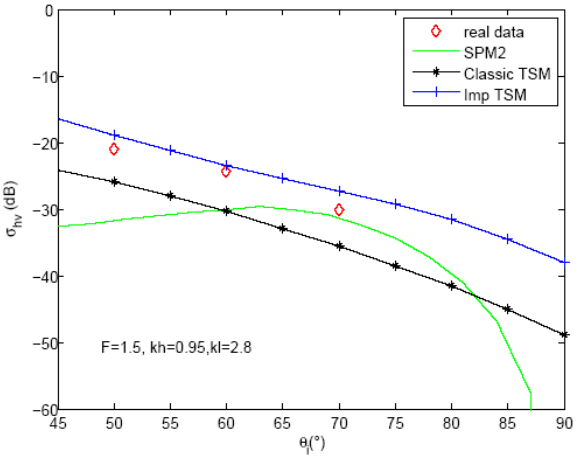

Figure 15. Comparison of Improved TSM with experimental data [18], SPM2 and classic TSM for cross polarization.

We have also done simulations with rms height set to 0.32 cm and 1.12 cm on L-band. From them and the above figures we observe that as the value of rms height increases the second order scattering effects by SPM2 contributes more to the intensity of σ_{pq}.

V. CONCLUSION

An improved model of TSM is studied with its application to sea surface and extended to bare soil surface. The validity of this model is examined through comparison with the published experimental data in monostatic configuration on Ku- and L band, for sea and soil surface as a function of incident angle. The new method gives better results for cross-polarizations as opposed to classical TSM, which is very important for the better retrieval of surface parameters. We also observe that as the roughness of sea and soil surface increases gradually (i.e., by choosing higher wind speeds for sea surface and larger value of rms height for soil surface), the model produces improved results for σ_{HH}. To make this model applicable in whole domain for all polarizations there are some issues to solve yet e.g., in specular domain fixing the scale dividing parameter ... for second order scattering. The work is in progress and we report these results later on.

REFERENCES

[1] J.A. Ogilvy, Theory of wave scattering from random rough Surfaces (Adam Higler, 1991).

[2] F. T. Ulaby, R. K. Moore, and A. K. Fung, Microwave Remote Sensing: Active and Passive, (Addison-Wesley Publishing Company, 1982), Vol. 2.

[3] F.T. Ulaby, C. Elachi, Radar polarimetry for geoscience applications (Artech house, norwood, MA, 1990).

[4] S.L. Broschat, E.I. Thorsos, A. Ishimaru, J. Electromag. Waves Appl. 3, 237 (1989).

[5] A. Khenchaf and O. Airiau, "Bistatic radar moving returns from sea surface," IEICE Trans. Elect. E83, 1827–1835 (2000).

[6] A. Khenchaf, "Bistatic scattering and depolarization by randomly rough surface: application to the natural rough surface in X-band," Waves in Random Media 11,61-87 (2001).

[7] A. Khenchaf, F. Daout, and J. Saillard, "The two-scale model for random rough surface scattering," in Prospects for the 21st Century, IEEE Proc. Oceans, 96, 50–54 (1996) [doi:10.1109/OCEANS.1996.568346].

[8] A. G. Voronovich, "Small-Slope Approximation in wave scattering by rough surfaces," Sov. Phys. JETP 62, 65–70 (1985).

[9] A. G. Voronovich, "Small-Slope Approximation for electromagnetic wave scattering at a rough interface of two dielectric half-spaces," Waves Random Media 4, 337–367 (1994) [doi:10.1088/0959-7174/9/4/304].

[10] Davidson, M., et al."A validation of multi-scale surfaces roughness dscription for the modelling of rdara backscattering from bare soils", I1 Intern. Work. on Retr. of Geo-physical Param. from SAR data for Land Applic., 21-23 Oct. 1998, Estec, The Netherlands

[11] Bass, F. Fuks, I. Kalmykov, A. Ostrovsky, I. Rosenberg, A."Very high frequency radiowave scattering by a disturbed sea surface Part II: Scattering from an actual sea surface", IEEE Trans. Antenna and Propagation, AP- 16(5), 560-568,1968.

[12] Wright, J.W., "A new model for sea clutter", IEEE Trans. Ant. Prop., vol. 16, issue 2, pp. 217-223, 1968.

[13] Yisok Oh, "Quantitative retrieval of soil moisture content and surface roughness from multipolarized radar observations of bare soil surfaces**,"** IEEE Transactions on Geoscience and Remote Sensing, Volume 42, Issue 3, March 2004 Page(s): 596 - 601.

[14] N. Sajjad, A. Khenchaf, A. Coatanhay and A. Awada, "An improved two scale model for the ocean surface bistatic scattering, IGARSS, Boston, USA, 6-11 july, 2008

[15] C. Cox andW. Munk, "Slopes of the sea surface deduced from photographs of sun glitter," Bull. Scripps. Inst. of Oceanog. 6, 401–488 (1956).

[16] T. Elfouhaily, B. Charpon, K. Katsaros: "A unified directional spectrum for long and short wind-driven waves", JGR, 102, 15781-15796, 1997

[17] W. J. Plant, "Microwave sea return at moderate to high incidence angles,"Waves in Random Media, vol. 13, no. 3, pp. 339-354, Oct. 2003.

[18] Yisok Oh, Kamal Sarabandi, and Fawwaz T.Ulaby, "An empirical model and an inversion technique for radar scattering from bare soil surfaces," IEEE Transactions on Geoscience and Remote Sensing, vol. 30, no. 2, pp. 370-381, March 1992.

[19] L. Tang and J. A. Kong, Scattering of Electromagnetic Waves, Vol. 3:Advance Topics, Wiley Interscience, 2001

[20] P. Debye. Polar molecules. Chemical cathalog compabny, New York, 1929.

[21] Moor, R. K.; Fung, A. K.,1979: "Radar determination of winds at sea, Proceedings of the IEEE, vol 67, no. 11, p. 1504-21